

COMPARATIVE DOSIMETRY OF BEIR VI REVISITED

Anthony C. James^{1,*}, Alan Birchall² and Gamal Akabani³

¹ACJ & Associates, Inc., 129 Patton Street, Richland, WA 99352, USA

²Dose Assessments Department, National Radiological Protection Board (NRPB), Chilton, Didcot, Oxon OX11 0RQ, UK

³Department of Radiology, Duke University Medical Center, Research Drive, Durham, NC 27710, USA

Received September 1 2003, accepted November 14 2003

The BEIR VI Committee applied recent developments in the comparative dosimetry of radon exposures in mines and homes to evaluate the so-called *K*-factor used to extrapolate the excess relative risk of lung cancer determined for underground uranium miners to exposures in homes. This paper describes methodological aspects of these developments that were specified ambiguously in the BEIR VI report. Specifically, in the section dealing with dosimetry (Appendix B of the BEIR VI report), the *K*-factor was unusually defined in terms of exposure to radon gas (K_{gas}), and not in terms of exposure to potential alpha energy (*K*). An incorrect value of unity was calculated for K_{gas} . This implies a value of 0.44 for *K*. In this paper, we describe how application of the ICRP Publication 66 lung and dosimetric models to evaluate the regional lung dose per unit exposure to potential alpha-energy in mines and homes yields the value of *K* = unity. This confirms the BEIR VI Committee's choice of *K* = 1 for application in their risk extrapolation model. The paper also reviews the use of doses to specific sub-cellular targets in the evaluation of *K*. This yields a somewhat greater divergence in the corresponding estimates of *K*, but again an overall average value of *K* = unity. The paper describes the methods used to calculate alpha particle hit probabilities for specific sub-cellular targets, and the resulting estimates of single- and multiple-hit probabilities obtained for exposures in mines and homes, as a function of the respective exposure rates.

INTRODUCTION

The purpose of this paper is to publish the technical basis for the newly developed comparative dosimetry of inhaled radon progeny that was cited and applied in the National Research Council's 1999 BEIR VI Report⁽¹⁾. In particular, we describe the application of the International Commission on Radiological Protection's 1994 ICRP Publication 66 lung model⁽²⁾ to evaluate doses to sensitive tissues in the lungs from radon progeny exposures in mines and homes, and the calculation of alpha-particle hit probabilities. The BEIR VI Committee's conclusions regarding typical exposure characteristics in underground uranium mines and homes are applied to derive characteristic estimates of both the radiation dose and hit probability for defined cellular targets in bronchial and bronchiolar epithelia. The targets considered are taken to represent the nuclei and cytoplasm of basal and secretory cells, respectively.

The National Research Council's previous report concerning the application of comparative dosimetry of radon progeny exposures for the purpose of extrapolating uranium miner risk estimates to domestic exposure was entitled 'Comparative Dosimetry of Radon in Homes and Mines'⁽³⁾. That (1991) report adopted the contemporary findings

'in progress' of the ICRP's Task Group on a Human Respiratory Tract Model for Radiological Protection. However, several of those preliminary findings were later refined by the Task Group for ICRP's recommended (1994) respiratory tract model⁽²⁾. As a result of these subsequent developments, the comparative dosimetry of inhaled radon progeny changed significantly. Of particular importance, newer data on the efficiency of the nose and mouth in filtering ultrafine radon progeny aerosols, and a more representative (lower) breathing rate for miners were incorporated in the ICRP Publication 66 respiratory tract model. These developments made it necessary for the BEIR VI Committee to re-evaluate for their 1999 report⁽¹⁾ the comparative dosimetry of radon progeny that was carried out in the 1991 NRC study⁽³⁾.

Appendix B of the BEIR VI report focused on the substantial developments in the quality of information on the range of radon progeny aerosol characteristics in mine and home atmospheres that have occurred since the 1991 NRC study. However, Cavallo⁽⁴⁾ noted that the *K*-factor had been unusually defined in terms of exposure to radon gas (K_{gas}) and not in terms of exposure to potential alpha energy (*K*). Since the conclusion of Appendix B was that $K_{\text{gas}} = 1$, this implies a value of *K* = 0.44. However, in the rest of the BEIR VI report, which extrapolates the risk from mine exposure to the risk from domestic exposure, a value of *K* = 1 was

*Corresponding author: consult@acj-associates.com

assumed. In this paper, the dosimetric information in BEIR VI is re-analysed, and a value of $K = 1$ is derived. This justifies BEIR VI's use of $K = 1$ in their risk projection models⁽¹⁾. The value of $K = 1$ is in agreement with that calculated by Marsh *et al*⁽⁵⁾ from European data.

THE 'K-FACTOR' INTRODUCED IN BEIR IV

The BEIR IV Committee⁽⁶⁾ introduced the formal concept of a dimensionless factor, K , that would serve to extrapolate the risk to miners per unit exposure to radon progeny potential alpha energy to that for an individual exposed in the home. On the assumption that 'risk' is proportional to 'dose', the National Research Council in their 1988 BEIR IV report⁽⁶⁾ defined K as follows:

$$K = \frac{\text{Risk}_h/\text{WLM}_h}{\text{Risk}_m/\text{WLM}_m} \propto \frac{\text{Dose}_h/\text{WLM}_h}{\text{Dose}_m/\text{WLM}_m} \quad (1)$$

where the subscripts 'h' and 'm' denote 'home' and 'mine', respectively, and, working level month (WLM) is the practical unit of exposure to radon progeny potential alpha energy that has been used as the common exposure metric in epidemiological studies of lung cancer in radon-exposed underground miners^(7,8). One WLM is defined as the exposure to 1 WL concentration of radon progeny potential alpha energy in air for 170 h (1 working month). The WL is defined as any combination of radon (or thoron) progeny in air that ultimately releases 1.3×10^5 MeV of alpha energy during decay⁽⁹⁾.

The 'WLM' was proposed as the metric of exposure (to radon progeny) that was most likely to be related to the 'dose' received by the lung tissues of underground miners, and thus, presumably, to an increased 'risk' of contracting lung cancer⁽⁹⁾. However, following several 'dosimetric' studies in the 1980s⁽¹⁰⁻¹⁵⁾, the BEIR IV Committee recognised that many additional factors (such as the particle size, the 'unattached' fraction, and the breathing rate of the exposed individual) would be expected to modify the amount of increased risk per 1 WLM exposure in both mines and homes. Thus, all such 'quantifiable' modifying factors are potentially taken into account in the evaluation of the characteristic 'dose conversion coefficient' (Dose/WLM) for both mines and homes, for substitution into Equation 1. From their review of the contemporary results of dosimetric modeling, the BEIR IV Committee were unable to select with confidence a specific value of K . Instead, they assumed that $K = \text{unity}$. Thus, BEIR IV did not 'scale' the risk projection parameter β in their recommended model for relating 'excess relative risk' (ERR) to past exposure to potential alpha energy over specified time periods.

THE 'K-FACTOR' USED FOR RISK EXTRAPOLATION IN BEIR VI

The BEIR VI Committee's risk projection models include some 'exposure' factors that were not considered in the BEIR IV model. However, the BEIR VI Committee used the K -factor defined by BEIR IV to 'scale' their miner-epidemiology-based risk models for exposure in homes. The BEIR VI Committee's risk models have the general form:

$$\text{ERR} = \beta(w_{5-14} + \theta_{15-24}w_{15-24} + \theta_{25+}w_{25+})\phi_{\text{age}}\gamma_{\zeta} \quad (2)$$

where the 'w' terms are the amounts of past exposure to potential alpha energy (in WLM) over the subscripted time intervals before death (from lung cancer), the ' θ ' weighting factors represent the assumed 'level of effect' assigned to each period of past exposure, and the ' ϕ ' factor is a function of age (at death), and the numerical subscripts denote ranges of age. The values of both β and γ_{ζ} depend on the specific form of the risk projection model used. For the so-called exposure-age-duration model, the BEIR VI Committee's recommended value of β_{ED} is approximately $0.5\% \text{ WLM}^{-1}$. For the so-called exposure-age-concentration model, the recommended value of β_{ER} is approximately $7.5\% \text{ WLM}^{-1}$.

The K -factor (as defined by Equation 1) is applied simply to scale the risk projection parameter β (both β_{ED} and β_{ER}), thus:

$$\beta_h = K\beta_m \quad (3)$$

In concordance with Equation 2, Appendix A of the BEIR VI report⁽¹⁾ defines the unit of the risk projection parameter β as WLM^{-1} , and generally expresses this as per cent WLM^{-1} . Since the BEIR VI Committee adopted the value $K = 1$ as being appropriate for men, women and children (age 10 y), with a marginally higher value of K for infants (age = 1), from Equation 3, the committee's risk projections for exposure in the home assumed in effect that $\beta_{\text{home}} = \beta_{\text{mine}}$ ⁽¹⁾. Thus, the numerical values of β (both β_{ED} and β_{ER}) derived from the underground miner studies were applied directly (with their respective risk model formulations) to calculate the range of ERR expected for radon progeny exposure in homes.

THE 'RADON EXPOSURE' METRIC IN HOMES

Appendix B of the BEIR VI report⁽¹⁾ recognised that the 'practical' metric of exposure in homes is the time-integrated radon gas concentration, and not the 'WLM'. It is the exposure rate that is measured in homes, as represented by the radon gas

COMPARATIVE DOSIMETRY OF BEIR VI REVISITED

concentration. The distribution of exposure rates for the US population is quantified in terms of the estimated distribution of mean radon gas concentration in homes. Thus, in order to project radon-attributable risks for the US population, it is necessary to relate domestic exposure, E_{Rn} (measured and expressed as $Bq_{Rn} h m^{-3}$) to the equivalent exposure to potential alpha energy, E_p (in WLM). These exposure quantities are related as follows:

$$E_p \text{ (in WLM)} = \frac{E_{Rn} \text{ (in } Bq_{Rn} h m^{-3}) \times F}{3700 (Bq_{Rn} m^{-3} WL^{-1}) \times 170 (h M^{-1})} \quad (4)$$

where F is the equilibrium factor relating the concentration of radon (^{222}Rn) gas in the home to the 'equilibrium equivalent' concentration, and M denotes the 'working month' (of 170-h duration). The BEIR VI Committee found the arithmetic average value of F to be 0.408. This was rounded to $F = 0.4$ for risk projection purposes. Therefore, from Equation 4, the annual exposure to potential alpha energy in the home can be expressed in terms of the mean radon gas concentration, \overline{C}_{Rn} , as follows:

$$w' \text{ (WLM } y^{-1}) = \overline{C}_{Rn} (Bq_{Rn} m^{-3}) \times 6.36 \times 10^{-7} \times (Bq_{Rn}^{-1} m^3 WL h^{-1} M) \times \Psi (h y^{-1}) \quad (5)$$

where Ψ is the number of hours per year spent in the home. The BEIR VI Committee recommended an 'occupancy factor' for the home of 0.7. Therefore, the value of Ψ is $6136 h y^{-1}$. The relationship between the annual exposure to potential alpha energy in the home and the mean radon gas concentration is therefore:

$$w' \text{ (in WLM } y^{-1}) = 3.9 \times 10^{-3} \times \overline{C}_{Rn} \text{ (in } Bq_{Rn} m^{-3}) \quad (6)$$

Equation 6 is used to evaluate the periodic 'potential alpha energy exposure' terms (w_{5-14} , w_{15-25} and w_{25+}) in which the BEIR VI Committee expresses the ERR from radon exposure in the home (see Equation 2)⁽¹⁾.

REFERENCE EXPOSURE CONDITIONS IN HOMES AND MINES

The BEIR VI Committee reviewed the currently available data on the activity-size distribution of radon (^{222}Rn) progeny aerosols in homes and mines. For homes, the Committee used the detailed measurements of activity-size distributions made with a six-stage graded-screen array⁽¹⁶⁾ that were reported by Hopke *et al.*⁽¹⁷⁾. The Committee recommended two characteristic activity-size distributions (as summarised in Tables 1 and 2). These were taken to represent homes without or with a cigarette smoker. In order to define these 'characteristic' data, the Committee selected the measured activity-size distribution that corresponded to the median calculated value of the dose rate per unit radon gas concentration from the population of samples for each of the two categories of home: a total of 422 samples from 4 homes without a cigarette smoker, and 143 samples from 2 homes with a single cigarette smoker in each home. The resulting characteristic values of the unattached fraction of potential alpha energy (f_p) were 15 and 8%, for the 'non-smoker' and 'smoker' homes, respectively. The corresponding values of the equilibrium factor (F) for these two 'characteristic' activity-weighted size distributions were 0.44 and 0.51.

In the case of underground uranium mines, the BEIR VI Committee used Knutson and George's⁽¹⁸⁾ 1992 re-evaluation of cascade impactor measurements made in the 1970s at 27 different locations in four large (diesel-operated) underground mines in New Mexico. The Committee characterised the ^{222}Rn progeny aerosol by considering data applicable to

Table 1. Characteristic activity-weighted size distribution of radon progeny aerosol in a 'non-smoker' home.^(a)

Median of logarithmic particle size interval (nm)	Fractional airborne activity concentration (%)			
	^{218}Po	^{214}Pb	^{214}Bi	PAEC ^(b)
0.9	30.8	14.6	11.3	15.0
2.8	3.4	2.4	1.8	2.3
8.9	3.9	2.4	3.4	2.9
28.1	12.8	10.8	1.3	11.8
88.9	23.1	30.0	28.6	28.6
281.2	26.0	40.2	41.9	39.4

^(a)Taken from the BEIR VI Report, Appendix B, Figure B-15

^(b)Potential alpha-energy concentration

Table 2. Characteristic activity-weighted size distribution of radon progeny aerosol in a ‘smoker’ home.^(a)

Median of logarithmic particle size interval (nm)	Fractional airborne activity concentration (%)			
	²¹⁸ Po	²¹⁴ Pb	²¹⁴ Bi	PAEC ^(b)
0.9	23.1	5.8	6.3	7.8
2.8	2.2	2.7	2.8	2.7
8.9	1.8	2.8	2.8	2.7
28.1	8.0	9.9	9.7	9.6
88.9	27.0	32.6	32.2	31.8
281.2	38.0	46.3	46.2	45.4

^(a)Taken from the BEIR VI Report, Appendix B, Figure B-16^(b)Potential alpha-energy concentration**Table 3. Characteristic activity-weighted size distribution of radon progeny aerosol in an underground uranium mine.**^(a)

Median of logarithmic particle size interval (nm)	Fractional airborne activity concentration (%)			
	²¹⁸ Po ^(b)	²¹⁴ Pb ^(b)	²¹⁴ Bi ^(b)	PAEC ^(c)
1.0	2.56	0.37	0.24	2.8
1.6	0.50	0.02	0.24	0.8
2.5	0.91	0.03	0.24	1.0
4.0	1.23	0.04	0.24	1.2
6.3	2.24	0.05	0.12	1.6
10.0	0.61	0.15	0.05	0.8
15.9	2.33	0.34	0.47	3.1
25.1	1.11	0.20	0.29	1.7
39.8	1.04	0.28	0.71	2.7
63.1	4.22	1.60	1.31	9.1
100.0	8.45	2.58	1.20	13.8
158.5	6.80	5.67	2.37	23.3
251.2	5.36	3.49	2.56	17.1
398.1	3.14	1.54	1.26	8.2
631.0	2.75	1.07	1.00	6.3
1000.0	3.26	0.99	1.06	6.4
Column total:	45 ^(b)	17 ^(b)	12 ^(b)	100

^(a)Derived here directly from the original⁽¹⁷⁾ data files (E. O. Knutson and A. C. George, pers. commun.). These data are to be compared with Figure B-17 of the BEIR VI Report, Appendix B^(b)Progeny activity concentrations are expressed as a fraction of the ²²²Rn activity concentration^(c)Potential alpha-energy concentration

four different work settings: (i) slushing sites, (ii) stopes, (iii) drifts and haulageways and (iv) machine shops. They assumed that the average fraction of the working shift spent by a miner in each of these work settings was 0.4, 0.4, 0.1 and 0.1, respectively. The summary data shown in Table 3 are the corresponding time-weighted mean activity-size fractions for the airborne ²²²Rn progeny. According to these data, the mean value of unattached fraction of potential alpha energy (f_p) is 2.8%, and the mean equilibrium factor (F) is 0.18. However, it should be noted that the value of F plays no part in the assessment of the corresponding ‘reference’ dose conversion coefficient (DCC), since the latter involves only

the measured potential-alpha-activity-weighted particle-size distribution. Thus, the measured radon gas concentration (and value of F) in these mines has no practical application.

APPLICATION OF THE ICRP PUBLICATION 66 DOSIMETRY MODEL

In order to evaluate dose conversion coefficients for the characteristic activity-weighted particle size distributions described above for homes and underground mines, we used the human respiratory tract model recommended by ICRP⁽²⁾. The fractional deposition in each region of the adult male respiratory

COMPARATIVE DOSIMETRY OF BEIR VI REVISITED

tract, that is, in the extrathoracic (ET), bronchial (BB), bronchiolar (bb) and alveolar-interstitial (AI) regions, was calculated for each median particle size shown in the first columns of Tables 1 and 2 (for homes) and Table 3 (for mines). The software code LUDEP vs. 2.0⁽²⁰⁾ was used to calculate the resulting regional deposition. For exposure in the home, we used the combinations of 'reference' breathing rates (sleep, rest and light exercise) recommended by ICRP⁽²⁾. This gave a mean ventilation rate of 0.779 m³ h⁻¹. For exposure in the mines, we used the combination of rest, light exercise and heavy exercise recommended to represent occupational exposure⁽²⁾. This gave a mean ventilation rate of 1.2 m³ h⁻¹ (slightly lower than the 1.25 m³ h⁻¹ assumed by the BEIR VI Committee). First, we assumed for all particle sizes considered that the particles were spherical, with unit density, and with no tendency for hygroscopic growth in the respiratory tract. Alternatively, we assumed that hygroscopic particle growth does occur in the respiratory tract: the assumption mentioned (and apparently used) by the BEIR VI Committee. To calculate regional lung deposition for 'hygroscopic' particles, we assumed that the size within the respiratory tract of all radon progeny associated with 'particles' was double the median size in ambient air, that is, twice the values given in Tables 1–3. For the unattached progeny, we assumed no hygroscopic growth⁽³⁾, that is, a constant size of 0.9 nm for exposure in the home and 1.0 nm for exposure in mines.

The resulting values of fractional regional deposition were written to separate data files to define three sets of 'reference' fractional respiratory tract deposition: for mines and homes ('non-smoking' and 'smoking'), respectively. A reduced version of the 15-airway-generation code developed for the NRC Comparative Dosimetry study⁽³⁾ was then used to read each of the reference deposition efficiency files, and to solve the ICRP Publication 66 mechanical clearance and absorption model⁽²⁾.

For these calculations we assumed that, upon deposition in the bronchial or bronchiolar airways, the radon progeny atoms are uniformly distributed throughout the thickness of the lining layers of mucus. Furthermore, based on the experimental data on the rate of absorption of ²¹²Pb from human and animal lungs^(21–23), we assumed that each of the individual short-lived radon progeny atoms (i.e., ²¹⁸Po, ²¹⁴Pb and ²¹⁴Bi) are 'absorbed' into the blood at a negligibly slow rate in comparison with their radioactive decay rates. The nominal value of the absorption rate substituted in the ICRP Publication 66 clearance model⁽²⁾ was 10 h, and the standard ICRP dosimetric assumption was made that there is no significant transfer and retention of the radionuclides in the epithelial tissue itself, that is the 'bound' fraction is zero.

In calculating the resulting equilibrium activities of each of the ²²²Rn progeny in each dosimetric region of the lungs, we applied the standard ICRP dosimetric assumption⁽²⁾ that the mucus is divided into two layers; a surface layer of mucous 'gel' which is propelled towards the throat on the tips of the beating cilia, and an underlying watery layer of mucous 'sol' in which the cilia beat. Half of the deposited progeny atoms are assumed to be uniformly mixed in the gel layer, and half in the sol layer, that is, the 'slow-cleared' fraction is taken to be 0.5 (for sub-micron sized particles). The corresponding rates of 'mechanical' clearance from the bronchial and bronchiolar 'regions' of the respiratory tract are 10 and 0.03 d⁻¹, respectively, for the bronchial gel and sol layers, and 2 and 0.03 d⁻¹, respectively, for the bronchiolar sol and gel. None of these mechanical clearance processes is sufficiently rapid to influence significantly the number of radioactive decays that occurs in each lung region.

The equilibrium rates of ²¹⁸Po and/or ²¹⁴Po alpha-disintegrations were calculated for each dosimetric region of the lungs, that is, the BB, bb and AI regions, during exposure to unit airborne concentration of each progeny nuclide (²¹⁸Po, ²¹⁴Pb or ²¹⁴Bi), as a function of thermodynamic particle diameter. The resulting absorbed dose rates to basal and secretory cell nuclei in the bronchi, secretory cell nuclei in the bronchioles and alveolar-interstitial tissue were calculated using the values of absorbed fraction (for ²¹⁸Po and ²¹⁴Po alpha disintegrations in mucus gel or sol, as appropriate) and target tissue masses (for the adult male) recommended by ICRP⁽²⁾.

For radiological protection purposes, the ICRP derives a so-called weighted equivalent dose to the lungs as a whole (denoted by H_{TH}) by weighting and summing the equivalent doses calculated for the constituent target tissues as follows:

$$H_{TH} = 0.333H_{BB} + 0.333H_{bb} + 0.333H_{AI} + 0.001H_{LNTH} \quad (7)$$

where H_{BB} is the average of the equivalent dose calculated for bronchial basal and secretory cell nuclei, H_{bb} is the equivalent dose calculated for the secretory cell nuclei in the bronchioles, H_{AI} is the equivalent dose calculated for the alveolar-interstitial tissue, and H_{LNTH} is the equivalent dose calculated for the thoracic lymph nodes. For inhalation of ²²²Rn progeny the lymph node dose is negligible. Therefore, the weighted equivalent dose to the lungs is in effect given by averaging the equivalent doses calculated for the BB, bb and AI regions (H_{BB} , H_{bb} and H_{AI}).

For the present purpose of comparing the dose conversion coefficient for exposure to ²²²Rn progeny in the home with that for exposure in a mine, we applied the same averaging procedure to

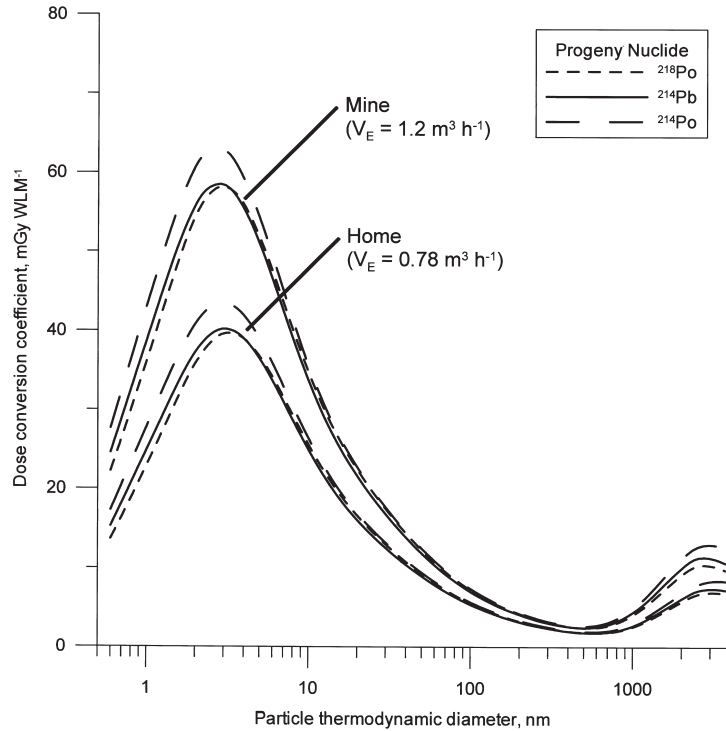


Figure 1. Dose per unit exposure to potential alpha energy (in mGy WLM^{-1}) calculated as a function of particle thermodynamic diameter. The average breathing rate, V_E , for exposure in a mine is $1.2 \text{ m}^3 \text{ h}^{-1}$, and that for exposure in homes is $0.78 \text{ m}^3 \text{ h}^{-1}$.

the absorbed doses calculated for each lung region. Figure 1 shows the resulting dose conversion coefficients calculated as a function of thermodynamic particle diameter for unit potential alpha energy exposure (1 WLM) to each of the ^{222}Rn progeny (^{218}Po , ^{214}Pb and ^{214}Bi) in a mine or a home. It should be noted that:

- the dose conversion coefficient is uniformly higher (for a given particle size) in a mine than it is in a home (because of the higher average breathing rate in the mine);
- there is very little difference between the dose conversion coefficients calculated for each individual progeny nuclide (hence the value of the ‘potential alpha energy’ as an indicator of dose, irrespective of the equilibrium factor).

Effect of particle size

Figures 2(a) and (b) compare the variation of the DCC calculated as a function of particle size with the BEIR VI Committee’s characteristic distributions of potential alpha energy concentration between the particle size ‘bins’ used to classify the radon progeny aerosol in homes. For this comparison we have re-classified the sixteen particle size bins used to

characterise the mine aerosol (Table 3) into the same six size bins used to characterise the home aerosols. In both parts of Figure 2, the first particle size bin (ranging in thermodynamic diameter from 0.6 to 1.6 nm) represents the classical ‘unattached’ ^{222}Rn progeny mode. The so-called unattached fraction, f_p , that is, the fraction of total potential alpha energy concentration (PAEC) in the ‘unattached’ mode, is 15% in the ‘non-smoking’ home, 8% in the ‘smoking’ home and only 2.8% in the mine atmosphere. The dose conversion factors (shown in both parts of Figure 2 for ^{214}Pb with the breathing rates appropriate for homes and mines, respectively) are approximately an order of magnitude higher for the ‘unattached’ mode than the corresponding values calculated for the classical sub-micron-sized ‘attached’ mode. However, the highest values of the DCC are not associated with these unattached ^{222}Rn progeny. Higher values apply to particles of between 2- and 10-nm thermodynamic diameter. These particles belong to the so-called nucleation mode^(1,16,24–27), which extends from about 2- to 30-nm thermodynamic diameter. The fraction of the PAEC in the nucleation mode is approximately 10% in all three reference atmospheres (mines, non-smoking and smoking homes). Therefore, coupled

COMPARATIVE DOSIMETRY OF BEIR VI REVISITED

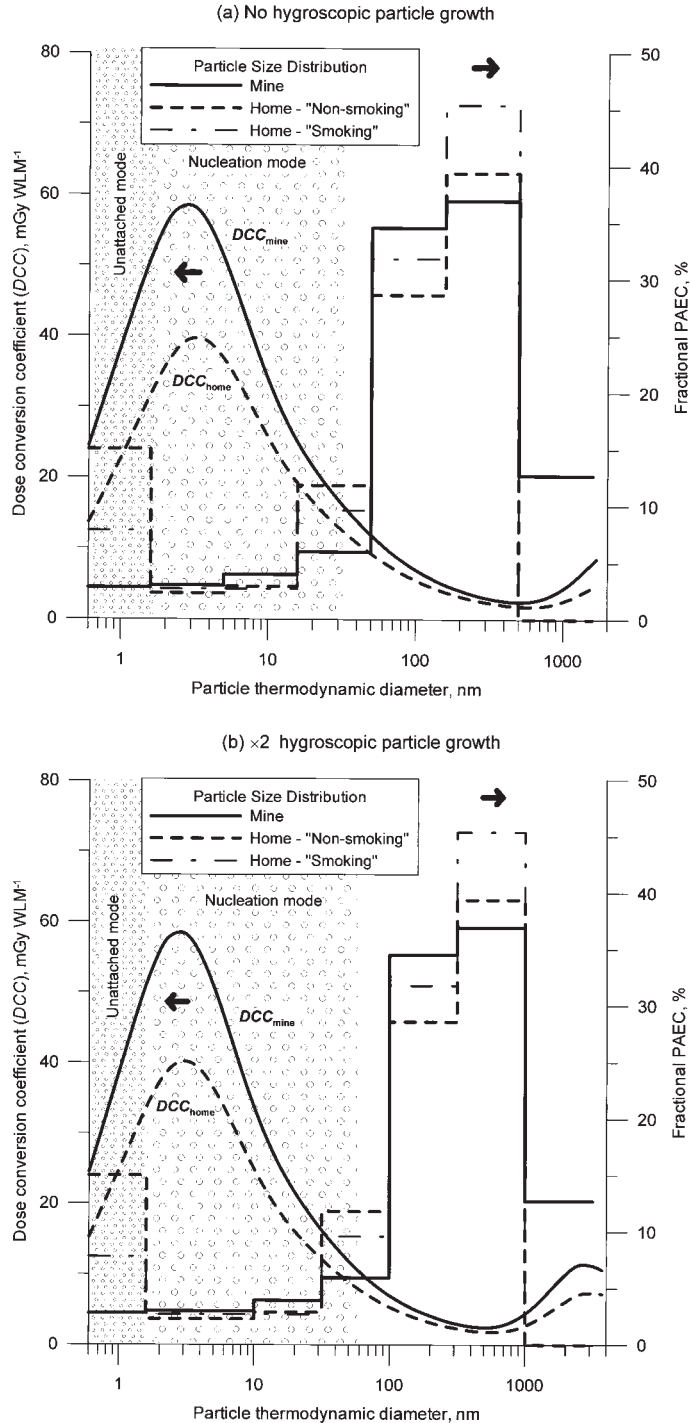


Figure 2. Activity-size distribution of potential alpha energy concentration (with the right-hand ordinate scale) compared for a mine, 'non-smoking' and 'smoking' homes: (a) assuming no hygroscopic particle growth, and (b) assuming two-fold hygroscopic particle growth in the respiratory tract. DCC calculated as a function of particle size (for exposure in mines and homes) are plotted on the same abscissa (with the left-hand ordinate scale).

Table 4. Indicator DCC and K -factors calculated for the typical conditions in mines and homes recommended in BEIR VI.

Exposure environment	DCC _{Lung} ^(a) (mGy WLM ⁻¹)	K_{Lung}	DCC _{Bb} ^(b) (mGy WLM ⁻¹)	K_{Bb}
<i>No hygroscopic growth</i> ^(c)				
Mine	8.7	—	12.8	—
Home				
Without cigarette smoke	8.9	1.0	13.1	1.0
With cigarette smoke	7.5	0.9	11.0	0.9
<i>2 hygroscopic growth</i> ^(c)				
Mine	7.4	—	10.9	—
Home				
Without cigarette smoke	8.8	1.2	13.1	1.2
With cigarette smoke	6.5	0.9	9.7	0.9

^(a)Dose per unit exposure to potential alpha energy averaged for all target cell nuclei in the lungs (bronchial (BB), bronchiolar (bb) and alveolar-interstitial (AI) regions)

^(b)Dose per unit exposure to potential alpha energy averaged only for target cell nuclei in the bronchi (B) and bronchioles (b)

^(c)Hygroscopic growth refers to the process of particle-size growth resulting from the adsorption of water molecules from the saturated air of the respiratory tract

with the substantially higher applicable DCC, the ‘nucleation’ mode in all three reference atmospheres is estimated to make a larger contribution to the total dose than the classical ‘unattached’ mode.

In both parts of Figure 2, the broad ‘peak’ in the particle size distributions (extending from 30- to 500-nm thermodynamic diameter in the absence of assumed hygroscopic growth in the respiratory tract) corresponds with the classical ‘attached’ particle mode. This is nowadays termed the ‘accumulation’ mode. Although the bulk of the PAEC is associated with this mode, the applicable values of the DCC for this mode are relatively low. Finally, the mine aerosol exhibits an additional ²²²Rn progeny particle-size mode, the so-called ‘coarse’ mode. This extends up to about 2- μ m thermodynamic diameter (in the absence of hygroscopic growth), and is probably associated with small particles of mineral ‘dust’. Note that the DCC increases quite sharply in this size-range, and so the ‘coarse’ mode does contribute to the overall dose in the mine environment.

The earlier exercises in comparative dosimetry between mines and homes^(3,14) did not take account of the presence of a significant amount of PAEC in the ‘nucleation’ mode. Through the late 1980s, the experimental techniques available to characterise ²²²Rn progeny activity-size distributions did not have sufficient resolution to discriminate the dosimetrically important nucleation mode.

Evaluation of the K -factor

By combining the DCC calculated above as a function of particle size with the ‘characteristic’ potential-alpha-energy-weighted particle size distributions

given in Tables 1–3, we obtained the overall dose conversion coefficients for the ‘mine’ environment and the ‘non-smoking’ and ‘smoking’ home environments given in Table 4. The table also shows the resulting values of the ‘ K -factor’ (given by Equation 1) for each home environment: under the alternative assumptions of (i) no hygroscopic particle growth or (ii) two-fold hygroscopic particle growth in the respiratory tract.

We evaluated the K -factor in two ways: (a) K_{Lung} was given by the quotient of the dose conversion coefficients (DCC_{Lung}) for homes and mines calculated by averaging the doses received by the bronchial, bronchiolar and alveolar-interstitial regions of the lungs (as is ICRP’s current practice for deriving a single weighted equivalent lung dose), and (b) K_{Bb} was given by the quotient of the corresponding DCC_{Bb} values (obtained by averaging just the bronchial and bronchiolar doses). It is seen from Table 4 that:

- The (rounded) K -factor varies from 0.9 (for a home with cigarette smoke, with or without assumed hygroscopic growth in the respiratory tract) to 1.2 (for a home without cigarette smoke but with assumed two-fold hygroscopic particle growth).
- The values of K_{Lung} and K_{Bb} are identical under the same exposure conditions. This is because the dose to the alveolar-interstitial region of the lungs is negligible compared to that received by the bronchi and bronchioles.
- Hygroscopic particle growth in the respiratory tract affects the value of the K -factor only for homes without cigarette smoke. However, the effect is small: an approximate 20% increase in

the K -factor for an assumed doubling of particle size.

Taking the average of the K -factors shown in Table 4 for both ‘non-smoking’ and ‘smoking’ home environments (under the likely bounds of zero to two-fold hygroscopic particle growth) gives an estimate of 1.0 for the overall K -factor. This confirms the BEIR VI Committee’s choice of $K = 1.0$ for application of their risk projection model to exposure, in terms of WLM, in homes. We did not calculate K -factors for women, children or infants, since these are not expected to be substantially different from the values calculated for the adult male^(1,3).

ALPHA PARTICLE HIT FREQUENCIES AND DOSES TO SPECIFIC CELLULAR TARGETS

In the words of the BEIR VI Committee, ‘There is good evidence that a single alpha particle can cause major genomic changes in a cell, including mutation and transformation. Even allowing for a substantial degree of repair, the passage of a single alpha particle has the potential to cause irreparable damage in cells that are not killed. In addition, there is convincing evidence that most cancers are of monoclonal origin, that is, they originate from damage to a single cell. These observations provide a mechanistic basis for a linear relationship between alpha-particle dose and cancer risk at exposure levels at which the probability of the traversal of a cell by more than one alpha particle is very small, that is, at exposure levels at which most cells are never traversed by even one alpha particle.’ Accordingly, BEIR VI examined the relationship between exposure rate and alpha-particle hit frequency in cellular targets (see Table 2-1 on p. 52 of Ref. (1)). In particular, the BEIR VI Committee used our computed alpha particle hit frequencies to indicate an approximate upper bound of exposure rate (among underground miners) at which carcinogenic response might be expected to become sub-linear with respect to potential alpha energy exposure.

The BEIR VI Committee compared alpha particle hit frequencies for various types of target cell in the lungs between exposures in mines and homes. They considered separately hits to nuclei and to the cytoplasm of basal and secretory cells. In order to calculate these hit frequencies for specific target shapes and dimensions, we developed the analytical method described in the Appendix to this paper. The resulting calculated values were summarised and discussed in the BEIR VI report⁽¹⁾ (Table 2-1). The analytical method used to evaluate alpha particle hit frequencies can also be used to evaluate the dose absorbed by these specific cellular targets.

The resulting ‘target specific’ dose factors can be used to define alternative expressions of the K -factor, as described below.

Cellular targets

The sizes of cellular targets assumed for the BEIR VI alpha particle hit frequency calculations were based on the morphological data reported by Geard *et al* (D. Brenner, Columbia University, NY, pers. commun.). Those authors represented the nucleus of a bronchial basal cell by a 5- μm diameter sphere, and that of a secretory cell by an ellipsoid with height 10 μm and diameter 5 μm . We assumed that the nucleus of a bronchial basal cell is incorporated in cytoplasm in the shape of a right circular cone, of height 10 μm and base diameter also 10 μm (Figure 3). To represent the bronchial secretory cell target, we assumed a cylindrical shape of height equal to the overall thickness of the epithelium, t_{BB} , and diameter 10 μm , as shown in Figure 3. Following ICRP Publication 66⁽²⁾, we assumed that in the bronchioles the sensitive target is the secretory cell. We represented the bronchiolar secretory cell by a 5- μm diameter spherical nucleus incorporated in cylindrical cytoplasm of height equal to the overall thickness of the bronchiolar epithelium, t_{bb} , and diameter 10 μm (as also shown in Figure 3).

The overall thickness of the bronchial epithelium determines the depth of the target cell nuclei below the radon progeny source, which is the superficial

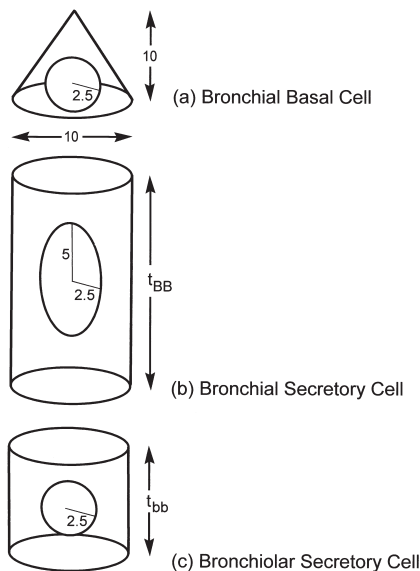


Figure 3. Diagram of three-dimensional cellular targets used to calculate dose and alpha particle hit probabilities. Dimensions are in μm .

Table 5. Depth distribution of cellular targets in bronchial epithelium.

Source of data	Depth to top of target (μm)			
	ICRP Publication 66 ⁽²⁾ (IC66)			Robbins <i>et al</i> ⁽²⁹⁾ (Ro90)
	Minimum	Typical	Maximum	Typical
Target				
Basal cell nuclei	35	40	45	20
Basal cell cytoplasm	31	36	41	16
Secretory cell nuclei	10	20	30	10
Secretory cell cytoplasm	—	0	—	0

layer of mucus. There is still substantial uncertainty about the characteristic thickness of the normal, healthy bronchial epithelium. Based primarily on the work of Mercer⁽²⁸⁾, the ICRP adopted a 'reference' overall thickness of 55 μm ⁽²⁾. However, Robbins *et al*⁽²⁹⁾ reported a significantly smaller value of about 30 μm for the thickness of normal bronchial epithelium. The corresponding variability in the estimated distributions of target depth below the epithelial surface (measured from the base of the cilia) is shown in Table 5 for the assumed overall epithelial thickness values of 55 or 30 μm . In contrast to the reported studies of bronchial epithelium, those of bronchiolar epithelial thickness are uniformly consistent with the reference value of 15 μm adopted in ICRP Publication 66⁽²⁾. The top of a bronchiolar secretory cell nucleus is typically about 6 μm beneath the epithelial surface, with a variation in depth from 4 to 7 μm .

Dose factors

The dose absorbed by cellular targets of specific shape and size is evaluated by first calculating for each mucous source (in bronchial and bronchiolar airways of assumed caliber 5 and 1 mm, respectively) the energy deposited in a 1- μm diameter spherical volume of tissue, at depth-intervals of 1 μm throughout the airway epithelium. The dose values at 1- μm intervals were then weighted by the fractional mass at each depth for each target shape, size and location. The resulting dose factors (in nGy per alpha-disintegration per unit area of airway wall) are given in Table 6. The dose factors were calculated specifically for the ²²²Rn progeny source in mucous gel or sol, and for both the bronchial and bronchiolar airway morphology described above.

It should be noted that the dose factors shown in Table 6 apply also for women, children and infants, since the morphometry (thickness and cellular composition) of the bronchial and bronchiolar epithelium is assumed to be independent of age and

gender.⁽²⁾ Only the airway caliber (and aerosol deposition characteristics) depend on age and gender. However, the calculated dose factor is insensitive to the airway caliber. Also, for inhaled ²²²Rn progeny, it has been shown before that the increased aerosol deposition efficiency and smaller surface areas of the airways in smaller subjects is balanced by their reduced ventilation rate. This yields an essentially invariant dose rate with age and gender for the same exposure to a given airborne ²²²Rn progeny concentration (for a given set of aerosol characteristics)^(3,30). Therefore, we did not evaluate doses to women, children or infants specifically for this paper.

Dose conversion coefficients

The above dose factors (values of dose per alpha disintegration of ²¹⁸Po or ²¹⁴Po) for the various cellular targets in bronchiolar and bronchial epithelium were multiplied by the calculated number of alpha disintegrations from ²¹⁸Po and ²¹⁴Po in each dosimetric region of the lung. This was done for all three reference exposure environments (the 'non-smoking' or 'smoking' home and the mine), to yield specific values of the DCC, that is, the total dose per unit exposure. The resulting values of the DCC are given in Tables 7 and 8, for the home and mine environments, respectively, and for each combination of cellular target and overall epithelial morphometry. These calculations assumed no hygroscopic particle growth, that is, they were performed for the reference fractional deposition values derived on the assumption of no hygroscopic particle growth in the respiratory tract.

K-factors

The DCC shown in Tables 7 and 8 for the home and mine, respectively, are expressed in the same units (mGy WLM⁻¹). Taking the quotient of each value in Table 7 and the corresponding value in Table 8 therefore gives an estimate of the K-factor for each

COMPARATIVE DOSIMETRY OF BEIR VI REVISITED

Table 6. Dose to cellular targets in bronchial and bronchiolar epithelium per single alpha disintegration of a ^{218}Po or ^{214}Po atom in mucous gel or sol.

Cellular target	Dose factor by nuclide for following source/target depth (nGy cm^{-2})							
	IC66 ⁽²⁾						Ro90 ⁽²⁹⁾	
	Maximum		Typical		Minimum		^{218}Po	^{214}Po
	^{218}Po	^{214}Po	^{218}Po	^{214}Po	^{218}Po	^{214}Po		
<i>Source in bronchial mucous gel</i>								
Basal cell nuclei	9.7	93	0.38	74	0	53	94	152
Basal cell cytoplasm	7.2	89	0.51	70	0.002	49	86	147
Secretory cell nuclei	147	187	75	141	19	102	147	187
Secretory cell cytoplasm	—	—	86	138	—	—	151	193
<i>Source in bronchial mucous sol</i>								
Basal cell nuclei	30	80	12	58	0.85	46	79	143
Basal cell cytoplasm	26	75	8.8	56	0.83	44	76	139
Secretory cell nuclei	128	180	71	132	39	90	128	180
Secretory cell cytoplasm	—	—	86	132	—	—	143	188
<i>Source in bronchiolar mucous gel</i>								
Secretory cell nuclei	265	271	243	255	233	248	243	255
Secretory cell cytoplasm	—	—	260	267	—	—	260	267
<i>Source in bronchiolar mucous sol</i>								
Secretory cell nuclei	260	266	238	249	227	241	238	249
Secretory cell cytoplasm	—	—	258	264	—	—	258	264

Table 7. DCC for targets in the bronchi and bronchioles from exposure to 1 WLM potential alpha energy in the home.^(a)

Target under following conditions	DCC (mGy WLM^{-1}) for following epithelial morphometry			
	IC66 ⁽²⁾			Ro90 ⁽²⁹⁾
	Maximum	Typical	Minimum	
<i>Without cigarette smoke</i>				
Bronchial basal cell nuclei	11.7	8.7	6.5	20.8
Bronchial basal cell cytoplasm	11.0	8.3	6.1	20.1
Bronchial secretory cell nuclei	26.3	19.1	13.1	26.3
Bronchial secretory cell cytoplasm	—	19.1	—	27.4
Bronchiolar secretory cell nuclei	13.2	12.3	12.0	12.3
Bronchiolar secretory cell cytoplasm	—	13.0	—	13.0
<i>With cigarette smoke</i>				
Bronchial basal cell nuclei	8.9	6.7	5.0	15.4
Bronchial basal cell cytoplasm	8.4	6.3	4.7	15.3
Bronchial secretory cell nuclei	20.0	14.5	9.9	20.6
Bronchial secretory cell cytoplasm	—	14.5	—	20.8
Bronchiolar secretory cell nuclei	12.2	11.4	11.1	11.4
Bronchiolar secretory cell cytoplasm	—	12.0	—	12.0

^(a) Assuming no hygroscopic particle growth in the respiratory tract

discrete cellular target. The resulting values of K are given in Table 9. For clarity of presentation, and to avoid the impression of undue precision, these values have been rounded to the nearest 0.05

increment. It is seen from Table 9 that:

- The calculated value of K depends very little on the assumed epithelial morphometry (thickness).

Table 8. DCC for targets in the bronchi and bronchioles from exposure to 1 WLM potential alpha energy in a mine.^(a)

Target	DCC (mGy WLM ⁻¹) for following epithelial morphometry			
	IC66 ⁽²⁾			Ro90 ⁽²⁹⁾
	Maximum	Typical	Minimum	
Bronchial basal cell nuclei	9.3	7.0	5.2	16.3
Bronchial basal cell cytoplasm	8.8	6.6	4.9	15.9
Bronchial secretory cell nuclei	20.8	15.1	10.4	21.1
Bronchial secretory cell cytoplasm	—	15.1	—	21.7
Bronchiolar secretory cell nuclei	15.5	14.5	14.1	14.5
Bronchiolar secretory cell cytoplasm	—	15.4	—	15.4

^(a)Assuming no hygroscopic particle growth in the respiratory tract

Table 9. Values of K -factor^(a) estimated for discrete cellular targets with alternative morphometric assumptions and by cigarette smoking status of the home.^(b)

Target under following conditions	K -factor for following epithelial morphometry	
	IC66 ⁽²⁾	Ro90 ⁽²⁹⁾
<i>Without cigarette smoke</i>		
Bronchial basal cell nuclei	1.25	1.30
Bronchial basal cell cytoplasm	1.25	1.25
Bronchial secretory cell nuclei	1.25	1.25
Bronchial secretory cell cytoplasm	1.25	1.25
Bronchiolar secretory cell nuclei	0.85	0.85
Bronchiolar secretory cell cytoplasm	0.85	0.85
<i>With cigarette smoke</i>		
Bronchial basal cell nuclei	0.95	0.95
Bronchial basal cell cytoplasm	0.95	0.95
Bronchial secretory cell nuclei	0.95	0.95
Bronchial secretory cell cytoplasm	0.95	0.95
Bronchiolar secretory cell nuclei	0.80	0.80
Bronchiolar secretory cell cytoplasm	0.80	0.80

^(a)Values rounded to nearest 0.05 increment

^(b)Assuming no hygroscopic particle growth in the respiratory tract

For the bronchi, ICRP Publication 66⁽²⁾ assumes an overall epithelial thickness of 55 μm , whereas Robbins *et al*⁽²⁹⁾ consider the thickness of bronchial epithelium to be only 30 μm .

- The value of K is lower for cellular targets in the bronchioles than it is for cellular targets in the bronchi.
- Assigning a 50% weight to each value of K calculated separately for bronchial basal and secretory cells (as is done by ICRP for the doses calculated separately), yields an overall average value of K of 0.95.

As discussed above in our analysis of the K -factor based on the recommended ICRP Publication 66⁽²⁾ regional dose factors (K_{Lung} and K_{Bb}), assuming

hygroscopic growth of particles in the respiratory tract would yield somewhat higher values of K for the home without cigarette smoke. Thus, our independent evaluation of K based on doses received by discrete cellular targets also supports the BEIR VI Committee's choice of $K = 1.0$ for application of their risk projection model to ²²²Rn progeny exposure in homes.

Evaluation of alpha particle hit probability

As described in the appendix, the probability that a particular target site is hit by an alpha particle in a given interval of time is estimated by the average dose received by that site divided by the mean event size. Tables 10 and 11 show the resulting estimates

COMPARATIVE DOSIMETRY OF BEIR VI REVISITED

Table 10. Mean daily hit probability for cellular target sites in the bronchi and bronchioles for exposure to a ^{222}Rn gas concentration of 1 kBq m^{-3} in homes.^(a)

Target under following conditions	Hit probability for following epithelial morphometry	
	IC66 ⁽²⁾	Ro90 ⁽²⁹⁾
<i>Without cigarette smoke</i>		
Bronchial basal cell nuclei	1.1×10^{-4}	2.6×10^{-4}
Bronchial basal cell cytoplasm	3.0×10^{-4}	7.4×10^{-4}
Bronchial secretory cell nuclei	4.1×10^{-4}	5.7×10^{-4}
Bronchial secretory cell cytoplasm	5.8×10^{-3}	4.9×10^{-3}
Bronchiolar secretory cell nuclei	1.5×10^{-4}	1.5×10^{-4}
Bronchiolar secretory cell cytoplasm	1.2×10^{-3}	1.2×10^{-3}
<i>With cigarette smoke</i>		
Bronchial basal cell nuclei	9.6×10^{-5}	2.4×10^{-4}
Bronchial basal cell cytoplasm	2.8×10^{-4}	7.1×10^{-4}
Bronchial secretory cell nuclei	3.9×10^{-4}	5.5×10^{-4}
Bronchial secretory cell cytoplasm	5.4×10^{-3}	4.6×10^{-3}
Bronchiolar secretory cell nuclei	1.8×10^{-4}	1.8×10^{-4}
Bronchiolar secretory cell cytoplasm	1.4×10^{-3}	1.4×10^{-3}

^(a)Daily hit probability calculated for a domestic occupancy factor of 0.7

Table 11. Mean daily hit probability for cellular target sites in the bronchi and bronchioles for exposure to a ^{222}Rn -progeny potential alpha energy concentration (PAEC) of 1 WL^(a) in mines.

Target under following conditions	Hit probability ^(b) for following epithelial morphometry	
	IC66 ⁽²⁾	Ro90 ⁽²⁹⁾
Bronchial basal cell nuclei	2.8×10^{-4}	7.0×10^{-4}
Bronchial basal cell cytoplasm	8.0×10^{-4}	2.0×10^{-3}
Bronchial secretory cell nuclei	1.1×10^{-3}	1.6×10^{-3}
Bronchial secretory cell cytoplasm	1.6×10^{-2}	1.3×10^{-2}
Bronchiolar secretory cell nuclei	6.4×10^{-4}	6.4×10^{-4}
Bronchiolar secretory cell cytoplasm	5.4×10^{-3}	5.4×10^{-3}

^(a)In SI units the PAEC is $20.8 \mu\text{J m}^{-3}$

^(b)Daily hit probability assumes an average occupancy factor of $\times 0.236$ to represent the working day (170 h per working month)

of the mean daily hit probability for the various cellular target sites considered in the bronchi and bronchioles, for the BEIR VI Committee's reference exposure conditions in homes and mines, respectively. For exposure in the home, it is assumed that the subject spends on the average 70% of his or her time in the home (Table 10). The hit probability values shown in Table 10 relate to an assumed average concentration of ^{222}Rn gas of 1 kBq m^{-3} . To represent the daily hit probabilities for a different value of the average ^{222}Rn gas concentration, the tabulated values are simply scaled in proportion to the concentration. For exposure in a mine, it is assumed that the subject spends on the average 23.6% of his time in the mine (Table 11), i.e. 170 h per working month. The hit probability

values shown in Table 11 for mine exposure relate to an assumed average concentration of ^{222}Rn progeny (expressed in terms of the potential alpha energy concentration, PAEC) of 1 WL. Again, the daily hit probabilities for a different value of the exposure concentration are simply scaled by the concentration. Likewise, the hit probabilities for an exposure time greater than 1 day are obtained simply by scaling in proportion to the exposure time.

Hit-probability per cell cycle

For illustrative purposes we assumed a typical cell cycle period of 30 day for epithelial cells. Table 12 shows the resulting estimated probabilities that

Table 12. Probability of a single alpha particle hit to cellular targets in the bronchi and bronchioles during a 30-d exposure period^(a) in homes at various ²²²Rn gas concentrations.

Target under following conditions	Single-hit probability (%) at following ²²² Rn gas concentration ^(b)					
	0.1 kBq m ⁻³		1 kBq m ⁻³		10 kBq m ⁻³	
	IC66 ⁽²⁾	Ro90 ⁽²⁹⁾	IC66 ⁽²⁾	Ro90 ⁽²⁹⁾	IC66 ⁽²⁾	Ro90 ⁽²⁹⁾
<i>Without cigarette smoke</i>						
Bronchial basal cell nuclei	0.036	0.090	0.36	0.89	3.5	8.2
Bronchial basal cell cytoplasm	0.10	0.25	1.0	2.5	9.2	20
Bronchial secretory cell nuclei	0.14	0.19	1.4	1.9	12	16
Bronchial secretory cell cytoplasm	1.9	1.7	16	14	27	31
Bronchiolar secretory cell nuclei	0.051	0.051	0.51	0.51	4.8	4.8
Bronchiolar secretory cell cytoplasm	0.42	0.42	4.0	4.0	28	28
<i>With cigarette smoke</i>						
Bronchial basal cell nuclei	0.033	0.081	0.33	0.80	3.2	7.5
Bronchial basal cell cytoplasm	0.096	0.024	0.95	2.4	8.7	19
Bronchial secretory cell nuclei	0.13	0.19	1.3	1.9	12	16
Bronchial secretory cell cytoplasm	1.8	1.5	15	13	29	33
Bronchiolar secretory cell nuclei	0.060	0.060	0.60	0.60	5.7	5.7
Bronchiolar secretory cell cytoplasm	0.048	0.048	4.6	4.6	30	30

^(a)The 30-d period may represent the typical cycle time for an epithelial cell

^(b)In traditional units, the concentrations shown are 2.7, 27 and 270 pCi l⁻¹

various target cell sites receive a single alpha particle hit over the 30-d cell cycle, as a function of the average exposure rate in a home (i.e. for exposure rates represented by average ²²²Rn gas concentrations of 0.1, 1 and 10 kBq m⁻³). The table also illustrates the influence of the assumed epithelial morphometry on the single-hit probability.

Table 13 shows the corresponding estimated probabilities that each of these target cell sites will receive multiple (two or more) alpha particle hits in the 30-d period. Under any particular condition, the probability that a target cell site receives a given number of hits is evaluated from the estimated mean hit-probability, assuming that the number of hits is distributed randomly, that is according to the Poisson distribution⁽³¹⁾. The probability (in %) that a given target cell site is not hit in the assumed 30-d period is given by subtracting the sum of the single- and multiple-hit probabilities given in Tables 12 and 13, respectively, from 100%. Tables 14 and 15 present the corresponding single- and multiple-hit probabilities, respectively, in a 30-d exposure period as a function of the exposure rate in a mine (i.e., for exposure rates of 1, 10 and 100 WL).

By plotting the calculated values of single- and multiple-hit probabilities as a function of exposure rate in mines and homes, we observed the following:

- For the nuclei or cytoplasm of basal cells, and the nuclei of secretory cells, the probability of a

single alpha particle hit (over a 30-d period) increases with the exposure rate, reaching a maximum value (37%) for exposure rates in the range 20–50 WL in mines.

- For mine exposure rates less than about 1 WL, the probability of a single alpha particle hit to these targets increases in direct proportion to the exposure rate.
- For the cytoplasm of secretory cells, however, the probability of a single alpha particle hit is maximum (37%) at the relatively low exposure rate of about 2 WL.
- An exposure rate on the order of 100 WL gives approximately 100% probability of multiple alpha particle hits to basal and secretory cell nuclei (which might be presumed lethal).
- For secretory cell cytoplasm, approximately 100% probability of multiple alpha particle hits occurs at a substantially lower exposure rate of approximately 20 WL.
- For exposure in the home, the maximum probability (37%) of a single alpha particle hit occurs at exposure rates of approximately 7 kBq(²²²Rn) m⁻³ for secretory cell cytoplasm, 50 kBq(²²²Rn) m⁻³ for the nuclei of secretory cells or the cytoplasm of basal cells, and at more than 100 kBq(²²²Rn) m⁻³ for the nuclei of basal cells.
- For the nuclei of bronchial secretory cells (or the cytoplasm of basal cells), the increase of single alpha particle hit probability is linear with

COMPARATIVE DOSIMETRY OF BEIR VI REVISITED

Table 13. Probability of multiple alpha particle hits to cellular targets in the bronchi and bronchioles during a 30-d exposure period^(a) in homes at various ²²²Rn gas concentrations.

Target under following conditions	Multiple-hit probability (%) at following ²²² Rn gas concentration ^(b)					
	0.1 kBq m ⁻³		1 kBq m ⁻³		10 kBq m ⁻³	
	IC66 ⁽²⁾	Ro90 ⁽²⁹⁾	IC66 ⁽²⁾	Ro90 ⁽²⁹⁾	C66 ⁽²⁾	Ro90 ⁽²⁹⁾
<i>Without cigarette smoke</i>						
Bronchial basal cell nuclei	6.5×10^{-6}	4.1×10^{-5}	6.5×10^{-4}	0.0040	0.063	0.38
Bronchial basal cell cytoplasm	5.2×10^{-5}	3.2×10^{-4}	0.0052	0.031	0.49	2.7
Bronchial secretory cell nuclei	9.9×10^{-5}	1.9×10^{-4}	0.0098	0.019	0.91	1.7
Bronchial secretory cell cytoplasm	0.019	0.014	1.7	1.3	59	50
Bronchiolar secretory cell nuclei	1.3×10^{-5}	1.3×10^{-5}	0.0013	0.0013	0.13	0.13
Bronchiolar secretory cell cytoplasm	8.8×10^{-4}	8.8×10^{-4}	0.086	0.086	6.7	6.7
<i>With cigarette smoke</i>						
Bronchial basal cell nuclei	5.4×10^{-6}	3.3×10^{-5}	5.4×10^{-4}	0.0033	0.053	0.31
Bronchial basal cell cytoplasm	4.6×10^{-5}	3.0×10^{-4}	0.0046	0.029	0.43	2.5
Bronchial secretory cell nuclei	8.7×10^{-5}	1.8×10^{-4}	0.0086	0.018	0.80	1.6
Bronchial secretory cell cytoplasm	0.017	0.012	1.5	1.1	55	46
Bronchiolar secretory cell nuclei	1.8×10^{-5}	1.8×10^{-5}	0.0018	0.0018	0.17	0.17
Bronchiolar secretory cell cytoplasm	0.0012	0.0012	0.11	0.11	84	8.4

^(a)The 30-d period may represent the typical cycle time for an epithelial cell

^(b)In traditional units, the concentrations shown are 2.7, 27 and 270 pCi l⁻¹

Table 14. Probability of a single alpha particle hit to cellular targets in the bronchi and bronchioles during a 30-d exposure period^(a) in mines at various ²²²Rn progeny concentrations (PAEC).

Target under following conditions	Single-hit probability (%) at following PAEC concentration					
	1 WL		10 WL		100 WL	
	IC66 ⁽²⁾	Ro90 ⁽²⁹⁾	IC66 ⁽²⁾	Ro90 ⁽²⁹⁾	IC66 ⁽²⁾	Ro90 ⁽²⁹⁾
Bronchial basal cell nuclei	0.83	2.1	7.7	17	36	26
Bronchial basal cell cytoplasm	2.3	5.7	19	33	22	1.5
Bronchial secretory cell nuclei	3.2	4.6	24	30	12	4.0
Bronchial secretory cell cytoplasm	30	26	4.0	7.9	7×10^{-18}	5×10^{-14}
Bronchiolar secretory cell nuclei	1.9	1.9	16	16	28	28
Bronchiolar secretory cell cytoplasm	14	14	32	32	0.00015	0.00015

^(a)The 30-d period may represent the typical cycle time for an epithelial cell

exposure rate up to a radon gas concentration of about 10 kBq m⁻³ (250 pCi l⁻¹), i.e. the probability of multiple hits is negligible. The slope of the single-hit probability vs. exposure rate curve decreases at higher concentrations.

Illustration of hit-probabilities as functions of exposure rate

Figures 4 and 5 illustrate by means of a three-dimensional surface the effects on alpha particle

hit probabilities of varying both the exposure rate and the depth of the target site beneath the epithelial surface. Figure 4 relates to exposure in mines, and Figure 5 to exposure in homes. In both cases, sub-figure (a) shows the variation of the single-hit probability, and sub-figure (b) the variation of the multiple-hit probability. The exposure rate increases from left to right in each figure, and the depth of the target site decreases from the front to the back. By superimposing the shapes of the respective surfaces in Figures 4 and 5, one can estimate that, in terms of equivalent distributions

Table 15. Probability of multiple alpha particle hits to cellular targets in the bronchi and bronchioles during a 30-d exposure period^(a) in mines at various ²²²Rn progeny concentrations (PAEC).

Target under following conditions	Multiple-hit probability (%) at following PAEC concentration					
	1 WL		10 WL		100 WL	
	IC66 ⁽²⁾	Ro90 ⁽²⁹⁾	IC66 ⁽²⁾	Ro90 ⁽²⁹⁾	IC66 ⁽²⁾	Ro90 ⁽²⁹⁾
Bronchial basal cell nuclei	0.0035	0.022	0.33	1.9	21	62
Bronchial basal cell cytoplasm	0.028	0.17	2.5	12	69	98
Bronchial secretory cell nuclei	0.053	0.11	4.4	8.4	84	95
Bronchial secretory cell cytoplasm	8.4	5.9	95	90	~100	~100
Bronchiolar secretory cell nuclei	0.018	0.018	1.6	1.6	57	57
Bronchiolar secretory cell cytoplasm	1.2	1.2	48	48	~100	~100

^(a)The 30-d period may represent the typical cycle time for an epithelial cell

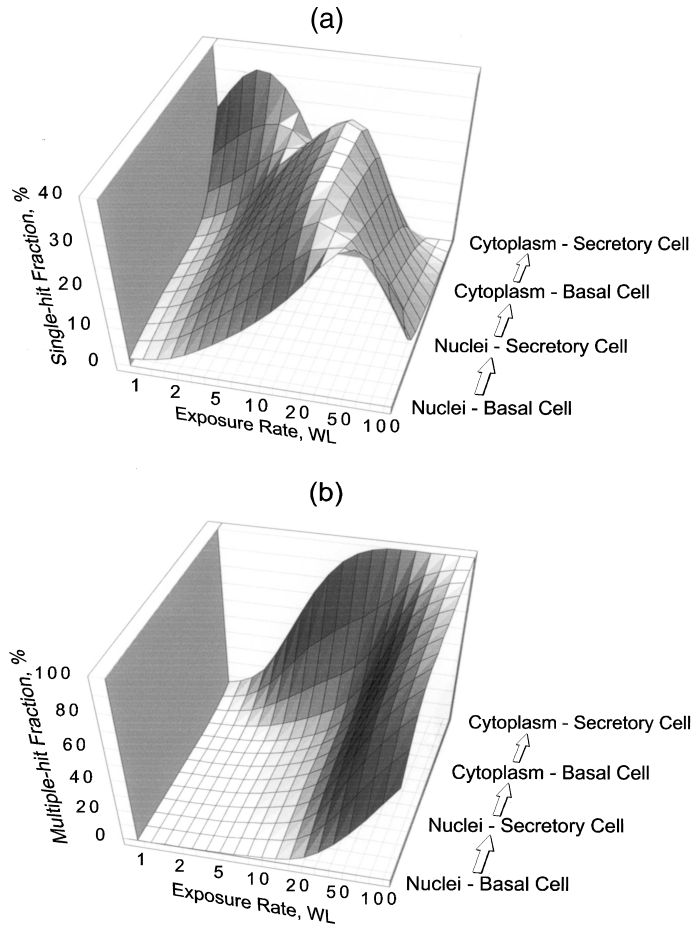


Figure 4. Fractions of cellular targets hit per 30-d exposure period (a) by a single alpha particle, or (b) by two or more alpha particles, as a function of the exposure rate (in WL) for the reference mine conditions. The three-dimensional surface illustrates the changes in hit-fractions as the mean depth of the target beneath the epithelial surface decreases, from the deep-lying basal cell nuclei through the secretory cell cytoplasm. The values of hit-fraction shown here are based on the target depths reported by Robbins *et al*⁽²⁹⁾.

COMPARATIVE DOSIMETRY OF BEIR VI REVISITED

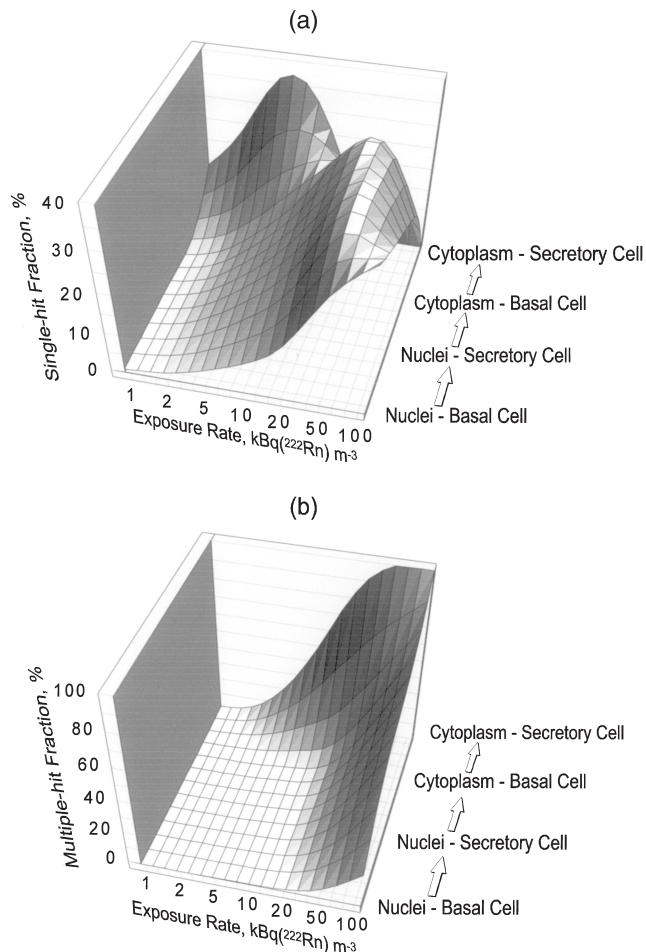


Figure 5. Fractions of cellular targets hit per 30-d exposure period (a) by a single alpha particle, or (b) by two or more alpha particles, as a function of the exposure rate (in $\text{kBq}^{(222\text{Rn})} \text{m}^{-3}$) for the reference home conditions (for comparison with Figure 4).

of hit-probability, exposure in a mine at a rate of 10 WL corresponds to exposure in a home at the rate of approximately $20 \text{ kBq}^{(222\text{Rn})} \text{m}^{-3}$. Therefore, on the basis of equivalence of target cell hit-probabilities, the currently recommended US Environmental Protection Agency (EPA) Action Level for ^{222}Rn gas concentration in US homes of 4 pCi l^{-1} (148 Bq m^{-3}) would correspond to a PAEC in mines of approximately 0.07 WL, and thus to an annual exposure rate in a mine of approximately 0.9 WLM y^{-1} . The corresponding probabilities of a single alpha particle hit to the nuclei of bronchial basal and secretory cells, and bronchiolar secretory cells (assuming a 30-d cell cycle, and ICRP Publication 66 bronchial epithelial morphometry) are 0.05, 0.2 and 0.1%, respectively.

CONCLUSIONS

From this re-examination of the comparative dosimetry applied by the BEIR VI Committee we draw the following conclusions:

- (1) Based on the average dose per unit exposure to ^{222}Rn progeny potential alpha energy received by bronchial and bronchiolar tissue (or the risk-apportioned average dose to the lungs as a whole), the BEIR VI Committee's adopted *K*-factor of unity is clearly appropriate.
- (2) The value of *K* based on these averaged doses is insensitive to the assumed thickness of bronchial epithelium (for which there are conflicting published estimates).
- (3) For the BEIR VI Committee's characteristic ^{222}Rn progeny aerosol conditions in mines and

- homes, the value of K is also insensitive to the assumed degree of hygroscopic particle growth within the saturated airways of the respiratory tract.
- (4) The value of K in a home with a cigarette smoker is marginally lower than that in a home without a cigarette smoker.
 - (5) The value of K is determined primarily by the potential alpha activity-weighted particle-size distributions that are assumed to characterise exposure in mines and homes.
 - (6) Although the data used by the BEIR VI Committee to characterise the mine aerosol were drawn from numerous and detailed measurements in four different underground uranium mines, these mines were all operated in the 1970s, and all with diesel equipment⁽⁴⁾. It has not been established how well these relatively modern mining conditions represent those in non-diesel mines of the 1950s and 1960s (in which much of the exposure of the underground miner cohorts occurred).
 - (7) The data used by the BEIR VI Committee to characterise the home aerosol were drawn from a very large number of individual samples taken from a small number of individual homes in the northeastern US (three homes in Princeton, NJ, one in Parishville, NY and one in Northfield, CT), and in one Canadian home (Arnprior, ON). It has not been established how representative the conditions in these homes are of other regions of the US (including the influence of seasonal and climatic conditions).
 - (8) Taking the BEIR VI Committee's characterisation of the ²²²Rn progeny aerosol conditions in mine and homes as the best currently available, consideration of doses to additional cellular targets, for example, the cytoplasm of secretory cells, rather than the 'regional' doses averaged only for cell nuclei in the ICRP Publication 66 dosimetry model, has the effect of increasing the range of calculated K values. The resulting range of K is about 0.80 for bronchiolar secretory cell cytoplasm as the target (in a home with cigarette smoke) to 1.25 for bronchial basal and secretory cells (nuclei and cytoplasm) in a 'non-smoking' home.
 - (9) The probability of a single alpha particle hit of a cellular target (which may be related to the probability of cancer induction) varies widely with both the selected target and the exposure rate.
 - (10) At low exposure rates, for exposure in both mines and homes, the probability of a single alpha particle hit increases linearly with exposure.
 - (11) At very high exposure rates, the probability of a single alpha particle hit decreases steeply with increasing exposure. The probability of multiple alpha particle hits (which may be related to cell lethality) can then be very high. For example, for an exposure rate of about 100 WL in a mine the probability of multiple alpha particle hits to both basal and secretory cell nuclei approaches 100% (on the assumption of a cell turnover time of about 30 d). However, the cytoplasm of secretory cells has approximately 100% probability of receiving multiple alpha particle hits at a lesser exposure rate of about 20 WL.
 - (12) Given the future development of a comprehensive mechanistic model of radon carcinogenesis, such analyses of alpha particle hit probability may prove to be helpful in evaluating the degree of linearity of the carcinogenic response to be expected as a function of exposure rate (and duration) in mines and homes.

ACKNOWLEDGEMENTS

This study was originally carried out in 1997 for the National Research Council's BEIR VI Committee under a Consulting Agreement with the National Academy of Sciences, as input to the Committee's deliberations. The original work has been updated and revised for publication under Contract Order No. 1W-1522-NASX between the USEPA Office of Radiation and Indoor Air (ORIA) and ACJ & Associates, Inc. The authors are grateful to Drs David Pawel and Jerome Puskin (ORIA) for many helpful discussions during the preparation of this paper.

REFERENCES

1. National Research Council. *Health Effects of Exposure to Radon: BEIR VI* (Washington, DC: National Academy Press) (1999).
2. International Commission on Radiological Protection. *Human Respiratory Tract Model for Radiological Protection*. ICRP Publication 66. Ann. ICRP **24**(1–3) (Oxford: Pergamon) (1994).
3. National Research Council. *Comparative Dosimetry of Radon in Mines and Homes* (Washington, DC: National Academy Press) (1991).
4. Cavallo, A. *The radon equilibrium factor and comparative dosimetry in homes and mines*. Radiat. Prot. Dosim. **92**, 295–298 (2000).
5. Marsh, J. W., Birchall, A. and Davis, K. *Comparative Dosimetry in Homes and Mines: Estimation of K-factors*. Presented at the Seventh International Symposium on the Natural Radiation Environment (NRE VII), 20–24 May, 2002, Rhodes, Greece (Proceedings in press).
6. National Research Council. *Health Risks of Radon and Other Internally Deposited Alpha-Emitters: BEIR IV* (Washington, DC: National Academy Press) (1988).

COMPARATIVE DOSIMETRY OF BEIR VI REVISITED

7. Lubin, J. H., Boice, J. D., Edling, C., Hornung, R. W., Howe, G., Kunz, E., Kusiak, R. A., Morrison, H. I., Radford, E. P., Samet, J. M., Tirmarche, M., Woodward, A., Yao, S. X. and Pierce, D. A. *Radon and Lung Cancer Risk: A Joint Analysis of 11 Underground Miner Studies*. National Institutes of Health, National Cancer Institute. NIH Publication No. 94-3644 (Washington DC: US Department of Health and Human Services) (1994).
8. Lubin, J. H., Boice, J. D., Edling, C., Hornung, R. W., Howe, G., Kunz, E., Kusiak, R. A., Morrison, H. I., Radford, E. P., Samet, J. M., Tirmarche, M., Woodward, A., Yao, S. X. and Pierce, D. A. *Radon-exposed underground miners and inverse exposure-rate (protracted enhancement) effects*. *Health Phys.* **69**, 494-500 (1995).
9. Holaday, D. A., Rushing, D. E., Coleman, R. D. *et al.* *Control of Radon and Daughters in Uranium Mines and Calculations on Biologic Effects*. DHEW Publication No. (PHS) 57-494 (Washington DC: US Department of Health, Education and Welfare) (1957).
10. Jacobi, W. and Eisfeld, K. *Dose to tissues and effective dose equivalent by inhalation of radon-222, radon-220 and their short-lived daughters*. GSF Report S-626 (Munich-Neuherberg, Germany: Gesellschaft für Strahlen-und Umweltforschung) (1980).
11. Harley, N. H. and Pasternak, B. S. *Environmental radon daughter alpha dose factors in a five-lobed human lung*. *Health Phys.* **42**, 789-799 (1982).
12. James, A. C., Jacobi, W. and Steinhäusler, F. *Respiratory Tract Dosimetry of Radon and Thoron Daughters: The State-of-the-art and Implications for Epidemiology and Radiobiology*. In: *Radiation Hazards in Mining: Control, Measurement and Medical Aspects*. Gomez, M., Ed. (New York, NY: Society of Mining Engrs) pp. 42-54 (1982).
13. Hofmann, W. *Cellular lung dose for inhaled radon decay products as a base for radiation-induced lung cancer risk assessment: I—Calculation of mean cellular doses*. *Radiat. Environ. Biophys.* **20**, 95-112 (1982).
14. Nuclear Energy Agency Group of Experts. *Dosimetry Aspects of Exposure to Radon and Thoron Daughter Products*. (Paris: Organization for Economic Cooperation and Development) (1993).
15. James, A. C. *Lung Dosimetry*. In: *Radon and Its Decay Products in Indoor Air*. Nazaroff, W. W. and Nero, A. V., Eds (New York, NY: John Wiley & Sons) pp. 259-309 (1988).
16. Ramamurthi, M. and Hopke, P. K. *An automated, semi-continuous system for measuring indoor progeny activity-weighted size distributions, dp: 0.5-500 nm*. *Aerosol Sci. Technol.* **14**, 82-92 (1991).
17. Hopke, P. K., Jensen, B., Li, C. S., Montassier, N., Wasiolek, P. T., Cavallo, A. J., Gatsby, K., Socolow, R. H. and James, A. C. *Assessment of the exposure to and dose from radon decay products in normally occupied homes*. *Environ. Sci. Technol.* **29**, 1359-1364 (1995).
18. Knutson, E. O. and George, A. C. *Reanalysis of data on particle size distributions of radon progeny in uranium mines*. In: *Indoor Radon and Lung Cancer: Reality or Myth?* Cross, F. T., Ed. (Columbus, OH: Battelle Press) pp. 149-164 (1992).
19. George, A. C., Hinchliffe, L. and Sladowski, R. *Size Distribution of Radon Daughter Particles in Uranium Mine Atmospheres*. Health and Safety Laboratory. HASL-326. (New York, NY: US Energy Research and Development Administration) (1977).
20. Jarvis, N. S., Birchall, A., James, A. C., Bailey, M. R. and Dorrian, M.-D. *LUDEP 2.0: Personal Computer Program for Calculating Internal Doses Using the ICRP Publication 66 Respiratory Tract Model*. NRPB-SR287 (Chilton, UK: National Radiological Protection Board) (1996).
21. International Commission on Radiological Protection. *Age-dependent Doses to Members of the Public from Intakes of Radionuclides: Part 4, Inhalation Dose Coefficients*. ICRP Publication 71. Ann. ICRP **25**(3-4) (Oxford: Pergamon) (1995).
22. Marsh, J. W. and Birchall, A. *Sensitivity analysis of the weighted equivalent lung dose per unit exposure from radon progeny*. *Radiat. Prot. Dosim.* **87**, 167-178 (2000).
23. Marsh, J. W. and Birchall, A. *Determination of lung-to-blood absorption rates for lead and bismuth that are appropriate for radon progeny*. *Radiat. Prot. Dosim.* **83**, 331-337 (1999).
24. Reineking, A., Butterweck, G., Kesten, J. and Porstendörfer, J. *Unattached fraction and size distribution of aerosol-attached radon and thoron daughters in realistic living atmospheres and their influence on radiation dose*. In: *Indoor Radon and Lung Cancer: Reality or Myth?* Cross, F. T., Ed. (Columbus, OH: Battelle Press) pp. 129-145 (1992).
25. Reineking, A., Knutson, E. O., George, A. C., Solomon, S. B., Kesten, J., Butterweck, G. and Porstendörfer, J. *Size distribution of unattached and aerosol-attached short-lived radon decay products: some results of intercomparison measurements*. *Radiat. Prot. Dosim.* **56**(1-4), 113-118 (1994).
26. Reineking, A., Porstendörfer, J., Dankelmann, V., and Wendt, J. *The size distribution of the unattached short-lived radon decay products*. In: *Radioaktivität in Mensch und Umwelt*. Winter, M., Henricks, K. and Doerfel, H., Eds (Lindau: Fachverband für Strahlenschutz e.V.) (1998).
27. Solomon, S. B., O'Brien, R. S., Wilks, M. and James, A. C. *Application of the ICRP's new respiratory tract model to an underground uranium mine*. *Radiat. Prot. Dosim.* **53**(1-4), 119-125 (1994).
28. Mercer, R. R., Russell, M. L. and Crapo, J. D. *Radon dosimetry based on the depth distribution of nuclei in human and rat lungs*. *Health Phys.* **61**, 117-130 (1991).
29. Robbins, E. S., Meyers, O. A. and Harley, N. H. *Quantification of the nuclei of human bronchial epithelial cells from electron micrographs for radon risk analysis*. In: *Proceedings of the XIIth International Congress for Electron Microscopy* (San Francisco, CA: San Francisco Press) (1990).
30. James, A. C. *Dosimetry of Inhaled Radon and Thoron Progeny*. In: *Internal Radiation Dosimetry*. Raabe, O. G., Ed. (Madison, WI: Medical Physics Publishing) pp. 161-180 (1994).
31. James, A. C. and Kember, N. F. *Alpha particle incidence in small targets*. *Phys. Med. Biol.* **15**, 39-46 (1970).

32. International Commission on Radiological Units. *Stopping powers and ranges for protons and alpha particles*. ICRU Report No. 49 (Bethesda, MD: ICRU Press) (1993).
33. Harley, N. H. *Spatial distribution of radon daughter and plutonium-239 alpha lung dose based on experimental energy absorption measurements*. Ph.D. Thesis (New York, NY: New York University) (1971).
34. James, A. C. *Dose to osteogenic cells from plutonium-239 deposited in rat bone*. *Radiat. Res.* **51**, 654–673 (1972).

APPENDIX

ICRP Publication 66⁽²⁾ provides values of the absorbed fraction of alpha particle energy, calculated as a function of emitted alpha particle energy, for the assumed ‘bands’ of depth beneath the epithelial surfaces that are occupied by the target cell nuclei in the bronchi and bronchioles. These depth bands constitute cylindrical shells of tissue extending, respectively, from 35 to 50 μm depth for bronchial basal cell nuclei, from 10 to 40 μm for bronchial secretory cell nuclei, and from 4 to 12 μm for bronchiolar secretory cell nuclei. The fraction of the emitted alpha energy absorbed by each band of target tissue defines the average dose absorbed by all target sites that are assumed to be uniformly distributed within each band. However, the BEIR VI Committee preferred to consider dose and alpha hit probabilities for individual cellular targets as a continuous function of depth in epithelial tissue. In order to evaluate these quantities in a tractable manner, this Appendix develops further the dosimetric methodology employed in Annex H of ICRP Publication 66⁽²⁾.

Dose calculation for specific cellular targets

The ICRP employed a Monte Carlo code to calculate absorbed fractions for cylindrical shells of target tissue. This incorporated the stopping power and range values for liquid water and air given on pp. 256 and 213, respectively, of *ICRU Report No. 49*⁽³²⁾. To calculate dose at a specific depth in tissue, Harley⁽³³⁾ used an analytical method: integration of an expression for the stopping power of ^{218}Po and ^{214}Po alpha particles as a function of distance traveled in tissue from each source element. A seventh-order polynomial expression was used to approximate the experimentally measured stopping power $(dE/dx)_x$, for alpha particles as a function of distance, x , in a tissue-equivalent medium:

$$\left[\frac{dE}{dx} \right]_x = [c_0 + c_1x + \dots + c_7x^7] \quad (\text{A1})$$

Harley then showed that, for an elemental volume of the alpha source (in a superficial layer of mucus), the rate of energy absorption, E' , in a spherical target of diameter, ρ , located in the airway wall at a radial distance, a , beneath the source element is given by:

$$E' = \int_0^{\cos^{-1}(a/R_{\max})} \frac{\rho^3 Q}{6a} [c'_0 + c'_1(a \sec \theta) + \dots + c'_7(a^7 \sec^7 \theta)] d\theta \quad (\text{A2})$$

where Q is the alpha activity per unit length of elemental volume (in $\text{s}^{-1} \mu\text{m}^{-1}$), ρ is the diameter of the target site (in μm), R_{\max} is the maximum range of the alpha particle in tissue, θ is the angle in the axial plane subtended at the target by the axial distance of the source element from the orthogonal radius, $d\theta$ is the increment of θ subtended by the source element, and $(a \sec \theta)$ is the distance, x , in tissue traveled by the alpha particle. The expression in square brackets is the polynomial approximation of the stopping power transformed for integration over the bounds of the angle θ .

Harley evaluated the definite integral (Equation A2) to obtain the total energy absorbed by a target site from a mucous source (cylindrical shell) of length greater than the alpha particle range. The integration is carried out in two parts: (i) for alpha particles originating in the ‘near’ wall (from which they reach the target by traveling entirely through tissue), and (ii) for alpha particles originating in the ‘far’ wall (from which they must cross the air-filled airway lumen).

Although a seventh-order polynomial provided a reasonable approximation of the experimental stopping power data, we found that this approximation did not accurately represent the ICRU-recommended (theoretical) values of alpha particle stopping power over the wider range of alpha particle energy from 10 keV to 10 MeV. For example, a seventh-order polynomial exhibits severe oscillation above about 7 MeV, and therefore is not reliable for high-energy alpha particles, for example, the 8.78-MeV ^{220}Rn (thoron) progeny nuclide ^{212}Po . To provide a generally applicable approximation of the alpha particle stopping power, it was necessary to increase the order of the polynomial to eleven. A formal parameter optimisation procedure [Graphically Interactive General Algorithm for FITting (GIGAFIT); A. Birchall, A. C. James, T. E. Hui, Pacific Northwest Laboratory, Richland, WA] was used to evaluate the polynomial coefficients in the expression:

$$\left[\frac{dE}{dx} \right]_{R_x} = c_0 + c_1 R_x + c_2 R_x^2 + \dots + c_{11} R_x^{11} \quad (\text{A3})$$

COMPARATIVE DOSIMETRY OF BEIR VI REVISITED

where $[dE/dx]_{R_x}$ is the total stopping power (in $\text{MeV } \mu\text{m}^{-1}$) for an alpha particle with residual range, R_x , the continuous slowing down approximation (CSDA) range (in μm) in liquid water. The fitted numerical values of the coefficients are given in Table A1. The resulting fit of this eleventh-order polynomial approximation of the ICRU-tabulated values of stopping power is shown in Figure A1. The approximation applies generally: for alpha particles of any energy between 10 keV and 10 MeV. This approximation was not improved by adding an additional (twelfth) order to the polynomial, that is, it is not possible to smooth the residual (relatively minor) oscillations shown in Figure A1 using a polynomial approximation.

To apply the ‘best-fit’ 11-order polynomial approximation of the alpha particle stopping power, Equation A2 must be expanded to 12 terms (with coefficients c'_0, \dots, c'_{11}). However, these coefficients c'_n relate to the tissue-equivalent distance, x , traveled by the alpha particle in reaching the target, and not to the residual range, R_x , of the alpha particle at the point of the target (as expressed in Equation A3). The fitted values of c_n must therefore be transformed to the equivalent values of c'_n (Equations A1 and A2) applicable for the two different energies of the ^{222}Rn progeny alpha particles. These are 6.00 MeV for ^{218}Po and 7.69 MeV for ^{214}Po . The required values of R_{max} were obtained (in μm as a continuous function of alpha particle energy, E_x , in MeV) by

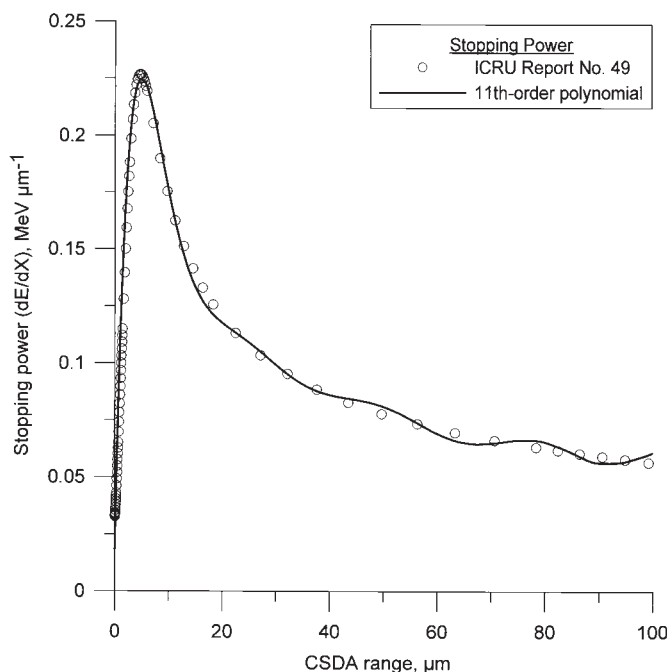


Figure A1. Eleventh-order polynomial fit to the values of stopping power as a function of CSDA range recommended by ICRU⁽³²⁾ for alpha particles in liquid water.

Table A1. Polynomial coefficients^(a) fitted to the stopping power of alpha particles in liquid water as a function of their residual CSDA range.

$c_0 = 1.7267882038998 \times 10^{-2}$	$c_4 = -1.1625576789533 \times 10^{-4}$	$c_8 = -1.3519562503660 \times 10^{-11}$
$c_1 = 1.1458603480764 \times 10^{-1}$	$c_5 = 3.9958292216170 \times 10^{-6}$	$c_9 = 8.4980927046771 \times 10^{-14}$
$c_2 = -2.2849661989601 \times 10^{-2}$	$c_6 = -9.0339789677024 \times 10^{-8}$	$c_{10} = -3.0610746483723 \times 10^{-16}$
$c_3 = 2.1385239995614 \times 10^{-3}$	$c_7 = 1.3609954581323 \times 10^{-9}$	$c_{11} = 4.8115302781620 \times 10^{-19}$

^(a)Fourteen significant figures are used to preserve computational accuracy for values of CSDA range $\geq 70 \mu\text{m}$

approximating the ICRU-tabulated values with the sum of two lognormal functions:

$$R_{\max}(E_x) = \frac{1}{\sqrt{2\pi}} \left\{ \frac{z_1}{\log_{10} \sigma_1} \exp \left[-\frac{(\log_{10} E_x - \log_{10} \mu_1)^2}{2(\log_{10} \sigma_1)^2} \right] + \frac{z_2}{\log_{10} \sigma_2} \exp \left[-\frac{(\log_{10} E_x - \log_{10} \mu_2)^2}{2(\log_{10} \sigma_2)^2} \right] \right\} \quad (\text{A4})$$

where $z_1 = 30.37$, $\sigma_1 = 44.0$, $\mu_1 = 24.2$, $z_2 = 2.33 \times 10^{16}$, $\sigma_2 = 3.178 \times 10^{16}$ and $\mu_2 = 90.13$. Thus, R_{\max} is 49.5 μm for the ^{218}Po alpha particle and 73.3 μm for ^{214}Po .

The sets of coefficients required for each of these progeny are given by substituting $(R_{\max} - x)$ for R_x in Equation A3. It can be shown that the coefficients c'_n of x (Equation A1) are given as a function of R_{\max} by:

$$c'_{11} = -c_{11} \quad (\text{A5})$$

$$c'_{10} = c_{10} + 11c_{11}R_{\max} \quad (\text{A6})$$

$$c'_9 = -c_9 - 10c_{10}R_{\max} - 55c_{11}R_{\max}^2 \quad (\text{A7})$$

$$c'_8 = c_8 + 9c_9R_{\max} + 45c_{10}R_{\max}^2 + 165c_{11}R_{\max}^3 \quad (\text{A8})$$

$$c'_7 = -c_7 - 8c_8R_{\max} - 36c_9R_{\max}^2 - 120c_{10}R_{\max}^3 - 330c_{11}R_{\max}^4 \quad (\text{A9})$$

$$c'_6 = c_6 + 7c_7R_{\max} + 28c_8R_{\max}^2 + 84c_9R_{\max}^3 + 210c_{10}R_{\max}^4 + 462c_{11}R_{\max}^5 \quad (\text{A10})$$

$$c'_5 = -c_5 - 6c_6R_{\max} - 21c_7R_{\max}^2 - 56c_8R_{\max}^3 - 126c_9R_{\max}^4 - 252c_{10}R_{\max}^5 - 462c_{11}R_{\max}^6 \quad (\text{A11})$$

$$c'_4 = c_4 + 5c_5R_{\max} + 15c_6R_{\max}^2 + 35c_7R_{\max}^3 + 70c_8R_{\max}^4 + 126c_9R_{\max}^5 + 210c_{10}R_{\max}^6 + 330c_{11}R_{\max}^7 \quad (\text{A12})$$

$$c'_3 = -c_3 - 4c_4R_{\max} - 10c_5R_{\max}^2 - 20c_6R_{\max}^3 - 35c_7R_{\max}^4 - 56c_8R_{\max}^5 - 84c_9R_{\max}^6 - 120c_{10}R_{\max}^7 - 165c_{11}R_{\max}^8 \quad (\text{A13})$$

$$c'_2 = c_2 + 3c_3R_{\max} + 6c_4R_{\max}^2 + 10c_5R_{\max}^3 + 15c_6R_{\max}^4 + 21c_7R_{\max}^5 + 28c_8R_{\max}^6 + 36c_9R_{\max}^7 + 45c_{10}R_{\max}^8 + 55c_{11}R_{\max}^9 \quad (\text{A14})$$

$$c'_1 = -c_1 - 2c_2R_{\max} - 3c_3R_{\max}^2 - 4c_4R_{\max}^3 - 5c_5R_{\max}^4 - 6c_6R_{\max}^5 - 7c_7R_{\max}^6 - 8c_8R_{\max}^7 - 9c_9R_{\max}^8 - 10c_{10}R_{\max}^9 - 11c_{11}R_{\max}^{10} \quad (\text{A15})$$

$$c'_0 = c_0 + c_1R_{\max} + c_2R_{\max}^2 + c_3R_{\max}^3 + c_4R_{\max}^4 + c_5R_{\max}^5 + c_6R_{\max}^6 + c_7R_{\max}^7 + c_8R_{\max}^8 + c_9R_{\max}^9 + c_{10}R_{\max}^{10} + c_{11}R_{\max}^{11} \quad (\text{A16})$$

The resulting values of these coefficients for the ^{218}Po and ^{214}Po alpha particles are substituted in Equation A2 (expanded to 12 terms). However, long-hand integration of this expanded equation is not tractable. Hence the following recurrence relationship was derived to evaluate the definite integral:

$$\begin{aligned} & \int (a \sec \theta)^n d\theta \\ &= a^n \int \sec^n \theta d\theta \\ &= a^n \left[\frac{1}{n-1} \frac{\sin \theta}{\cos^{n-1} \theta} + \frac{n-2}{n-1} \int \sec^{n-2} \theta d\theta \right] \\ &= \frac{a^n \sin \theta}{(n-1)\cos^{n-1} \theta} + \frac{(n-2)a^2}{n-1} \int (a \sec \theta)^{n-2} d\theta \end{aligned} \quad (\text{A17})$$

Denoting this integral by $I(n)$:

$$I(n) = \frac{a^n \sin \theta}{n-1 \cos^{n-1} \theta} + \frac{(n-2)a^2}{n-1} I(n-2) \quad (\text{A18})$$

Having expressed the integral $I(n)$ recursively in terms of $I(n-2)$, this can be evaluated for any n given the boundary conditions $I(0)$ and $I(1)$. It is readily shown that:

$$I(0) = \theta \quad (\text{A19})$$

and

$$I(1) = a \ln \left[\frac{1 + \sin \theta}{\cos \theta} \right] \quad (\text{A20})$$

Table A2 shows that the values of absorbed fraction calculated by this analytical method for various combinations of mucous source and target tissue region (as defined in ICRP Publication 66⁽²⁾) are consistent with the corresponding ICRP-tabulated values for the alpha emitting ^{222}Rn progeny [which were obtained by stochastic (Monte Carlo) calculation].

To confirm the accuracy of the above analytical method for calculating the average dose absorbed by targets of specific shape, and thus the adequacy of the eleventh-order polynomial fit to the stopping power data given in ICRU Publication 49⁽³²⁾, we used the tabulated stopping powers directly in a Monte Carlo simulation to evaluate the average dose to a 5- μm diameter spherical target as a function of depth below the epithelial surface from the disintegration (7.69 MeV alpha energy) of one ^{214}Po atom per cm^2 of airway surface. Figure A2 shows good agreement between the analytical and Monte Carlo methods of dose calculation.

Calculation of hit probability

The number of alpha particle 'hits' that would correspond to a particular calculated value of dose for

COMPARATIVE DOSIMETRY OF BEIR VI REVISITED

Table A2. Comparison of absorbed fractions calculated by the analytical method used in this study with the values calculated by the Monte Carlo method used for ICRP Publication 66 (Annexe H).⁽²⁾

Source/target regions	IC66		This study	
	²¹⁸ Po	²¹⁴ Po	²¹⁸ Po	²¹⁴ Po
Bronchial gel → Basal cell nuclei	0.00506	0.0893	0.00738	0.0908
Bronchial gel → Secretory cell nuclei	0.249	0.353	0.258	0.355
Bronchial sol → Basal cell nuclei	0.0217	0.0857	0.0232	0.0765
Bronchial sol → Secretory cell nuclei	0.272	0.355	0.252	0.332
Bronchiolar gel → Secretory cell nuclei	0.214	0.172	0.214	0.174
Bronchiolar sol → Secretory cell nuclei	0.217	0.173	0.210	0.170

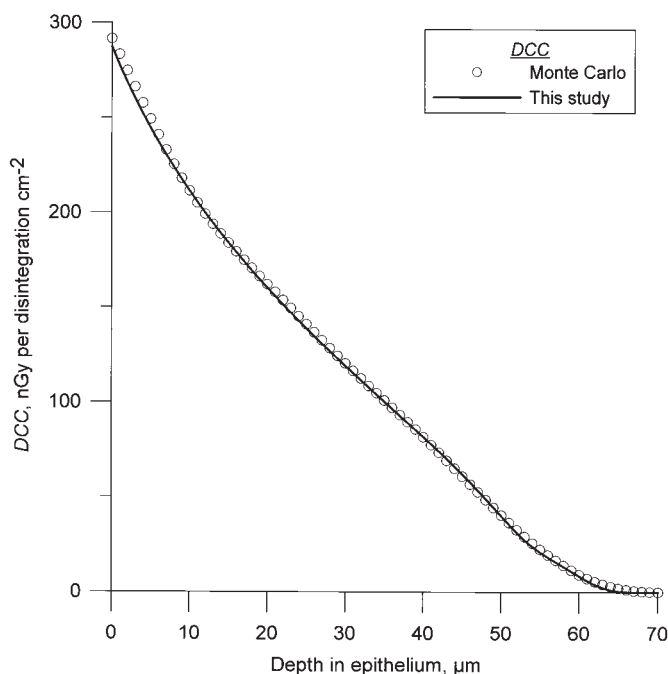


Figure A2. Comparison of the *DCC* calculated analytically or by the Monte Carlo method for a single ²¹⁴Po alpha disintegration per cm² airway surface and a 5-μm-diameter spherical target as a function of depth beneath the epithelial surface in the bronchi.

a specific cellular target was estimated by first determining a ‘characteristic’ event-size for ²¹⁸Po and ²¹⁴Po alpha particles traversing each target shape⁽³⁴⁾. Two simplifying assumptions were made: (i) that the event size is independent of the depth of the target below the mucous source and (ii) that the mean event size is reasonably well approximated by the product of the mean chord length for isotropically incident radiation and the track-average linear energy transfer (LET). The characteristic single-event sizes thus obtained for the various cellular

targets and airway wall morphometry considered in the paper are given in Table A3. In reality, the mean single-event size for each target is influenced by both the variation of alpha particle LET with the depth of the target in the airway wall, and, for non-spherical targets, by the departure from radiation isotropy at each depth.

The degree of approximation introduced into the estimation of hit probabilities by the simplifying assumption of a constant event size (dose per single hit) is illustrated in Figure A3. It is seen

Table A3. Assumed dimensions of target tissue sites with calculated average alpha-track traversal length (mean chord length) and corresponding average dose per single hit (single event size) for ^{218}Po and ^{214}Po alpha particles.

Target tissue site	Target dimension			Average chord length (μm)	Size of single event (Gy)	
	Radius (μm)	Height (μm)	Volume (μm^3)		^{218}Po	^{214}Po
<i>Bronchial basal cells</i>						
Spherical nucleus	2.5	5	65.4	3.33	0.985	0.852
Conical Cytoplasm	5	10	261.8	4.44	0.328	0.284
<i>Bronchial secretory cells</i>						
Ellipsoidal nucleus	2.5	10	130.9	3.90	0.577	0.499
Cylindrical cytoplasm:						
IC66 ⁽²⁾	5	55	4319.7	9.17	0.0411	0.0355
Ro90 ⁽²⁹⁾	5	30	2356.2	8.57	0.0704	0.0609
<i>Bronchiolar secretory cells</i>						
Spherical nucleus	2.5	5	65.4	3.33	0.985	0.852
Cylindrical cytoplasm:						
IC66 ⁽²⁾	5	15	1178.1	7.5	0.123	0.107
Ro90 ⁽²⁹⁾	5	15	1178.1	7.5	0.123	0.107

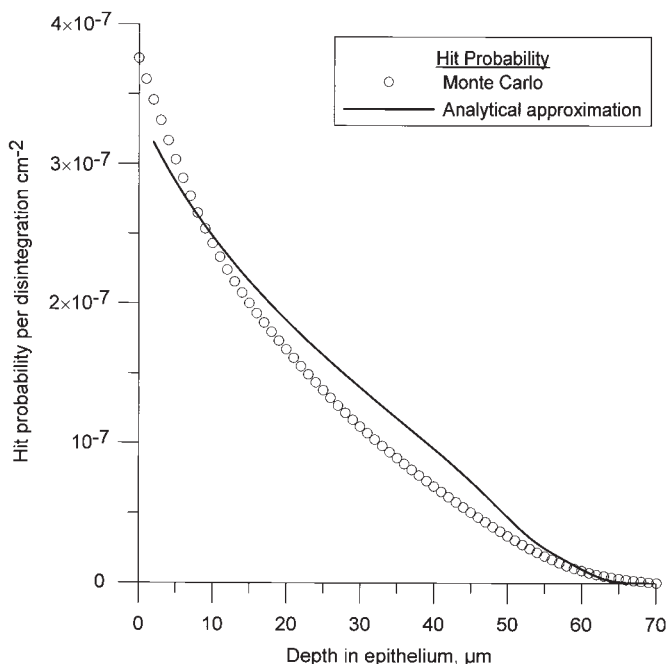


Figure A3. Comparison of the hit probability calculated accurately by the Monte Carlo method for a single ^{214}Po alpha disintegration per cm^2 airway surface and a 5- μm -diameter spherical target as a function of depth beneath the epithelial surface in the bronchi with the values estimated from the analytical calculation of absorbed dose by assuming a constant event size (0.852 Gy per hit).

that, at least for a 5- μm diameter spherical target, the error introduced into the estimated hit probability is relatively small (i.e. not more than about 40% of the true value). For targets at

depths of between 10 and 60 μm in the (bronchial) epithelium, the hit probability is marginally overestimated by this approximate method of calculation.